Earth and Planetary Science Letters 430 (2015) 171–177

Contents lists available at ScienceDirect

Earth and Planetary Science Letters

www.elsevier.com/locate/epsl

Weakly coupled lithospheric extension in southern Tibet

Xiaobo Tian [a,b,*], Yun Chen [a], Tai-Lin Tseng [c], Simon L. Klemperer [d], Hans Thybo [e], Zhen Liu [a,f], Tao Xu [a,b], Xiaofeng Liang [a], Zhiming Bai [a], Xi Zhang [a], Shaokun Si [g], Changqing Sun [h], Haiqiang Lan [a], Erchie Wang [a,b], Jiwen Teng [a]

[a] State Key Laboratory of Lithospheric Evolution, Institute of Geology and Geophysics, Chinese Academy of Sciences, Beijing 100029, China
[b] CAS Center for Excellence in Tibetan Plateau Earth Sciences, Beijing 100101, China
[c] Department of Geosciences, National Taiwan University, Taipei 10617, Taiwan
[d] Department of Geophysics, Stanford University, Stanford, CA 94305, USA
[e] Department of Geography and Geology, University of Copenhagen, DK-1350 Copenhagen K, Denmark
[f] University of Chinese Academy of Sciences, Beijing 100049, China
[g] Department of Deep-sea Investigation, National Deep Sea Center, State Oceanic Administration, Qingdao 266061, China
[h] Key Laboratory of Crustal Dynamics, Institute of Crustal Dynamics, China Earthquake Administration, Beijing 100085, China

ARTICLE INFO

Article history:
Received 15 April 2015
Received in revised form 11 August 2015
Accepted 19 August 2015
Available online 28 August 2015
Editor: A. Yin

Keywords:
Tibetan plateau
E–W extension
N–S trending rift
VDSS
crustal structure

ABSTRACT

West–east extension is a prominent tectonic feature of southern and central Tibet despite ongoing north–south (N–S) convergence between India and Eurasia. Knowledge of deep structure beneath the N–S trending rifts is key to evaluating models proposed for their origin, including gravitational collapse, oblique convergence along the arcuate plate boundary, and mantle upwelling. We model direct *S* and Moho-reflected *SsPmp* phases at teleseismic distances to constrain variations in crustal thickness across the major rifts crossed by a ~900-km long, W–E broadband array in the Lhasa Terrane. Crustal thicknesses are ~70–80 km. However, Moho depth decreases by ~10 km within a horizontal distance of 100 km west of the Yadong–Gulu rift (YGR) and Nyainquentanghla mountains (NQTL). This Moho uplift, taken with deep, extensional focal mechanisms and reduced seismic velocity in the upper mantle, suggests that asthenospheric upwelling has significantly contributed to the pattern of extension across the YGR and NQTL. The ~100-km separation between surface rift and Moho uplift is likely enabled by partial decoupling across a ductile middle crust.

© 2015 The Authors. Published by Elsevier B.V. This is an open access article under the CC BY-NC-ND license (http://creativecommons.org/licenses/by-nc-nd/4.0/).

1. Introduction

The Tibetan plateau was created by continental collision between India and Eurasia and their ongoing subsequent convergence (e.g., Molnar and Tapponnier, 1978). Observations from focal mechanisms in the upper crust (Copley et al., 2011), Quaternary and active faulting (Armijo et al., 1986), and geodetic deformation (Chen et al., 2004) all indicate that the tectonic regime includes a marked component of normal faulting and eastward extrusion in southern Tibet. The relationship between N–S shortening, uplift, and E–W crustal extension is fundamental to the mechanics of this collisional orogen (England and Houseman, 1989).

The development of N–S trending rifts in southern Tibet began in mid-to-late Miocene as the result of extension or eastward extrusion (e.g., Armijo et al., 1986). These rifts are regularly distributed, each a few hundred kilometers long and about 200 km apart, extending north from the Himalayas (Yin, 2000) (Fig. 1). The rifts are more prominent south of the Bangong–Nujiang suture (BNS) than further north (Armijo et al., 1986). Their orientations exhibit an axis of symmetry trending ~N10°E along ~87°E (Kapp and Guynn, 2004). Many rifts in southern Tibet cut across the Indus–Yarlung suture (IYS), with the Yadong–Gulu rift (YGR) at ~89°E and North Lunggar rift (NLR) at ~83°E, extending furthest south into the Himalayan range. These two rifts have undergone more total extension than the others (e.g., Chen et al., 2004), and GPS geodesy shows that one-half to two-thirds of the permanent extension between 80°E and 91°E is concentrated across the YGR (Chen et al., 2004).

Based on the absence of significant normal faulting in all areas of the plateau with mean elevation less than 4500 m, Molnar and Tapponnier (1978) proposed that the rifts result from gravitational spreading of upper crust induced by crustal over-thickening or by rapid uplift of the plateau due to delamination (down-welling)

* Corresponding author at: State Key Laboratory of Lithospheric Evolution, Institute of Geology and Geophysics, Chinese Academy of Sciences, Beijing 100029, China. Tel.: +86 10 8299 8329; fax: +86 10 8299 8001.
E-mail address: txb@mail.iggcas.ac.cn (X. Tian).

http://dx.doi.org/10.1016/j.epsl.2015.08.025
0012-821X/© 2015 The Authors. Published by Elsevier B.V. This is an open access article under the CC BY-NC-ND license (http://creativecommons.org/licenses/by-nc-nd/4.0/).

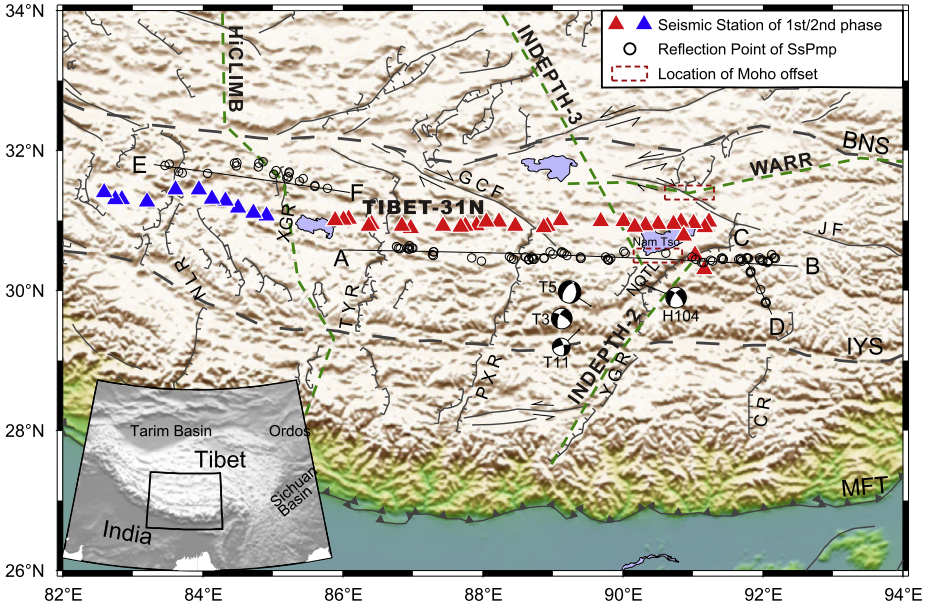

Fig. 1. Tectonic and topographic map of southern Tibetan plateau with seismic broadband stations used in this study. Red and blue triangles are the first and second phases of observation, respectively. Open circles mark *SsPmp* reflection points used in this study. Lines labeled AB, CD and EF are segments along which we construct Moho geometry. Green dashed lines represent N–S arrays of HiCLIMB, INDEPTH 2–3 and the E–W profile of wide-angle reflection–refraction (WARR) from Selin Tso to Yaanduo. Purple dashed rectangles mark the locations of Moho offset from Zhang and Klemperer (2005) and this study. Four focal mechanisms are the intermediate-depth earthquakes in southern Tibet (T3, T5 and T11 from Chen and Yang (2004) and Zhu and Helmberger (1996); H104 from Baur (2007), for parameters see Table S4). We show major thrust faults (MFT: Main Frontal Thrust), sutures (BNS: Bangong–Nujiang suture, IYS: Indus–Yarlung suture), strike-slip faults (GCF: Gyaring Co fault, JF: Jiali fault), and south–north trending rifts (CR: Comei rift, YGR: Yadong–Gulu rift, PXR: Pumqu–Xianza rift, TYR: Tangra Yum Co rift, XGR: Xiang–Gangjiang rift, NLR: North Lunggar rift). NQTL: Nyainquentanghla range. Geological structures from Taylor and Yin (2009). An west-dipping normal fault on the western side of the southern NQTL from Kapp et al. (2005) and Kidd et al. (1988).

of the lithospheric mantle (e.g., Molnar et al., 1993). This gravitational collapse model implies that the age of initiation of the rifts should be a proxy for the timing that Tibet achieved its maximum elevation (e.g., Harrison et al., 1992; Molnar et al., 1993). In contrast McCaffrey and Nabelek (1998), noting similarities between the Himalayan arc and subduction along curved oceanic trenches, suggested W–E extension on rifts in the southern Tibet and Himalaya results from oblique convergence along an arcuate margin. In this model, the normal faulting should only occur as far north as the underthrust Indian lithosphere provides a basal shear force (cf. Copley et al., 2011), and the faulting should not continue from the upper crust down into the underthrust plate. McCaffrey and Nabelek (1998) suggested that rifting can occur at any elevation, and that rift initiation is not a proxy for uplift of the plateau. In a third model, Yin (2000) emphasized the broad similarities in the history of volcanism, the age of rift initiation, and the trend and direction of extension of rifts in Tibet, Lake Baikal, and Shanxi. He proposed that all of eastern Asia experienced mantle upwelling beginning at ~40–35 Ma leading to thermal weakening of the lithosphere and eventual rift development at ~8–4 Ma. W–E extension was preceded and accompanied by ultrapotassic N–S trending dikes and adakitic intrusives in southern Tibet implying a magma source in the lithospheric mantle that also triggered melting of an eclogitic lower crust (Hou et al., 2004). Clearly, understanding the structure of the lower crust and uppermost mantle will shed light on the origin of the N–S trending rifts and the E–W extension.

The Lhasa block, bounded by the BNS to the north and IYS to the south (Fig. 1), is an ideal place to investigate the lateral variations of the deep structure beneath and between the rifts. We operated a 900-km-long west–east passive-source linear seismic array (TIBET-31N) along latitude ~31°N in the central Lhasa block, from the Lunggar range to Nam Tso, crossing several major N–S trending rifts (Fig. 1). The seismic array is divided into three segments. Segments AB and CD, composed of 48 and 10 seismographs, respectively, recorded during the first phase of deployment from September 2009 to November 2010 (Chen et al., 2015; Zhang et al., 2013). Segment EF including 13 seismographs was deployed from April 2011 to November 2011. All stations used in this study are also shown in Fig. S1 with station names.

2. Data, methods and results

In this study, we use the method of virtual deep seismic sounding (VDSS) developed by Tseng et al. (2009) to investigate the structure of the crust and uppermost of mantle beneath TIBET-31N. Unlike conventional seismic profiling with manmade sources near the surface, VDSS utilizes the conversion of teleseismic *S*- to *P*-wave at the free surface (near the receiver) as a virtual seismic source. The seismic phase *SsPmp* originates as the direct *S*-wave reflects at the free surface and partially converts to a *P*-wave that, in turn, reflects off the Moho before finally arriving at a seismic station. VDSS produces large, clear reflections that are insensitive to details of the Moho transition, thus providing a robust estimate of overall crustal thickness. For the simple case of a uniform crustal layer over a mantle half-space, the differential time between *SsPmp* and *Ss* arrivals is

$$T_{SsPmp\text{-}Ss} = 2H\left(1/V_P^2 - p^2\right)^{1/2}$$

where p is the ray-parameter (horizontal slowness) of the incoming *S*-wave, H the crustal thickness, and V_P the *P*-wave speed in the crust.

Among numerous earthquakes that occurred during each phase of the deployment, we choose large to moderate-sized events between epicentral distance of 30° and 50° for which the amplitude of the relevant seismic phases is expected to be large. Some stations have insufficient data due to power problems, including T_C11, T_C13 and T_C14, and are not shown in Figs. 1 and S1. Deep and shallow earthquakes are used in the analysis (Table S1).

Download English Version:

https://daneshyari.com/en/article/6427923

Download Persian Version:

https://daneshyari.com/article/6427923

Daneshyari.com